

RESEARCH

Open Access



Laboratory Investigation into the Flexural Behavior of Embedded Concrete Sleepers in Two-Stage Concrete with Preplaced Ballast Aggregate

Morteza Esmaili* and Hamid Amiri

Abstract

The conversion of ballasted railway tracks into slab tracks using the preplaced aggregate concrete (PAC) technology over the bridges and in the tunnels has been introduced by many researchers but the flexural behavior of this composite system has not yet been studied. Therefore, in the first stage, a series of mortar and concrete mixture designs were proposed and evaluated. Subsequently, a concrete beam mold with dimensions of 3 * 0.6 * 0.5 m, which represented the track conditions, was developed and the bending behavior of the constructed beams in both conditions of the presence and absence of the concert B70 sleeper were investigated. The maximum bending force in the middle of the concrete beam without a sleeper (SE) equaled 177.5 kN. In addition, the average values of bending tolerance by the sleeper including a PAC beam for three specimens in the four modes of the positive moment of midspan (SPM), negative moment of midspan (SNM), positive moment of rail seat (SPR), and negative moment of rail seat (SNR) were 55.25 kN m, 32.5 kN m, 91.84 kN m, and 38.21 kN m, respectively, which met the requirements of the AREMA regulations.

Keywords: ballasted tracks, ballast maintenance, preplaced aggregate concrete beam, bending behavior, ballastless track

1 Introduction

The railway track system generally consists of rails, fasteners, sleepers, a ballast, a sub-ballast, and a subgrade. As trains pass through the railway track, repetitive loading is imposed on the intact system which leads to the gradual breakdown of the ballast. In general, the maintenance of ballasted railway tracks seems to be more important than that of non-ballasted ones, because the former is prone to altered track geometrical parameters such as asymmetry, torsion, and distortion due to their flexibility and high ballast contamination. Usually, in

ballasted tracks, a significant portion of the track maintenance costs is annually spent on ballast cleaning and tamping. However, because of the increase in traffic congestion, some restrictions such as insufficient time for minor repairs and the inability to close the track for ballast maintenance activity will emerge. One of the problems associated with ballasted tracks is maintaining the ballast layer in bridges and tunnels. It is not possible to use common maintenance machinery in tunnels with a small gabarit due to the lack of proper ventilation. As a result, traditional methods have to be used to repair the ballast layer in tunnels, which are time-consuming and expensive. In bridges, the limited workspace and the generally manual substructure maintenance, as well as their time-consuming and costly nature, are the most notable restrictions. One method adopted to solve this problem is

*Correspondence: M_esmaeli@iust.ac.ir
School of Railway Engineering, Iran University of Science and Technology,
Tehran, Iran
Journal information:ISSN 1976-0485 / eISSN 2234-1315

the conversion of ballasted tracks into slab tracks via the injection of mortar into the ballast layer, which is called a paved track system based on the preplaced aggregate concrete (PAC) technology.

PAC refers to a kind of concrete in which ballast is first placed in the formwork; then, the mortar is injected into the ballast layer using compressor pressure. PAC was first used in 1937 by Lee Turzillo and Louis S. Wertz to repair a railroad tunnel in California. This method of concreting was only observed in the bridge and tunnel repairing process. Afterwards, it was employed to rebuild the Hoover Dam overflow and then, in 1946, in upstream dam repairs in Colorado. US army engineers also utilized this method in 1951, 1954, and 1955, when 3,333,000 m³ worth of concreting volume was used to build 34 bridges.

In railway engineering, this method has been widely applied in Japan and Australia since 1950 to convert ballasted tracks into slab tracks (Hagio, 2011). Because, in ballasted tracks, the initial stage of this method, which is the placement of aggregates, has been previously performed, so the entire system can be converted into slab tracks via the injection of mortar. This new technology has been employed in countries such as South Korea and Japan. Table 1 presents a short history of slab tracks executed by PAC technology. Fig. 1 displays an example of a track made of PAC in the Seoul metro.

In the laboratory environment, several tests have been developed and conducted on PAC and its mortar in different research works. For instance, Abdelgader et al. (2018) investigated the elastic behavior of PAC as sustainable production and showed an enhancement in terms of compressive strength, splitting tensile strength, and modulus of elasticity, compared to conventional concrete (CC). Coo et al. studied the effects of aggregates on the mechanical properties of preplaced aggregate mortar and concrete. They found that mortar workability is reduced as more sand is incorporated into the mixture, but the presence of sand helps the mortar to enhance its mechanical characteristics such as strength. The larger particle size of aggregates and their angular shape provide more



Fig. 1 Urban rail with PAC (Seoul metro) (Takahashi et al., 2012).

viscosity, while the interlocking between the aggregates increases the mortar resistance against loading (Coo & Pheerapahn, 2015). Moreover, Rajabi et al. developed the empirical formulas between PAC compressive strength and its geomechanical properties, compared to CC. They concluded that PAC compressive strength, tensile strength, and modulus of elasticity are larger than those of CC, but its Poisson's ratio is smaller (Rajabi & Moaf, 2017). Abdul Awal (1984) reported that the compressive strength of PAC is higher than that of CC in older ages, whereas its bleeding and creep are much lower. Abdelgader et al. investigated the behavior of PAC in underwater structures. They concluded that, in such conditions, PAC meets less particle segregation and drying shrinkage in comparison with structures constructed using CC, while it can achieve proper compressive and splitting tensile strength (Abdelgader et al., 2010). Moreover, Najjar et al. examined the durability and crack mechanism of PAC and reported that PAC possesses higher durability and lower tendency to crack generation compared to CC due to its increased cement-to-aggregate ratio and its advantageous trait for filling aggregate voids because of mortar fluidity (Najjar, 2016). Najjar et al. (2014) have

Table 1 Railway tracks with PAC (Hagio, 2011).

Project title	Location of operation	Operation year	Operated track length (km)
Phase 1	Japan (Tabata-Shinjuku-Tamachi)	1998	35
Phase 2	Japan (Tabata-Tokyo-Tamachi)	2002	111
Phase 3	Japan (Tokyo metro)	2007	182
–	South Korea Urban Railway	2003	–
–	South Korea (Seoul metro)	2007	–
–	South Korea (Busan-Yangsan metro track 2)	2009	–

an overview on the properties and applications of PAC and the effect of various factors such as: water to cement ratio, types of admixtures, rounded coarse aggregates, etc. Rajabi et al. (2020) indicated that the compressive strength, tensile strength, Young's modulus, ultrasonic pulse velocity, and Schmidt hammer rebound number were greater for PAC than for CC. Najjar et al. (2016) explored the rheological and mechanical properties of two-stage concrete made with single, binary and ternary binders and proposed an empirical equation between the modulus of elasticity and its compressive strength of PAC. In 2020, Mohammadhosseini et al. (2020) investigated the enhancement of strength and transport properties of a novel preplaced aggregate fiber-reinforced concrete by adding waste polypropylene carpet fibers, but the capacity of PAC beams is not yet known against bending and shear forces.

Lee et al. examined the effects of polymer powder on the mechanical and durability properties of PAC. They found that adding polymer would maximize the PAC tensile strength and minimize its ultimate shrinkage strain. They also proved that this material can improve the PAC property against freeze–thaw cycles (Lee et al., 2018). In conventional slab track systems, a minimum temperature reinforcement should be used to control system shrinkage in both directions (ACI318, 2011). On the other hand, in PAC, the coarse aggregates are first placed into the formwork, where they interact with one another. Therefore, the void imprisoned between the aggregates is filled using mortar to adhere to the aggregates and transmit the imposed force. This causes the PAC to perform well in compression and tension condition and, subsequently, the PAC slab will not require bending reinforcement, because PAC has a specific stress distribution mechanism at which the stresses are transferred through contact areas between aggregate particles. These stresses can be responsible for the fracture and tearing of aggregate particles away from the grout (Abdelgader & Górski, 2003; O'Malley & Abdelgader, 2010). In other words, the most noteworthy advantage of this new method of concreting is the omission of steel reinforcement which leads to a significant decrease in slab construction cost. The construction of this type of slab track can sharply minimize railway track maintenance time, is environmentally friendly, and limits the costs. Although a review of the literature on PAC applications in the railway superstructure demonstrates the substantial profits of this new system for ballast stabilization and its conversion to the slab system, no investigation has been conducted on the mechanical performance of the system. Since the bending capacity of slab beams constructed by PAC technology plays a vital role in their performance as a railway superstructure system, it is crucial to investigate PAC

beams under direct shear and moment applications. Consequently, the present study was allocated to the laboratory investigation of this issue. For this purpose, herein, mortar samples were first constructed to obtain the optimum mortar mixture design from both high-strength and low-fluidity standpoints, using silica sand prepared from Firuzkuh quarry and Portland cement type 1–425 manufactured in Tehran Cement Company. Afterward, using the developed injection apparatus, the PAC cylindrical concrete specimens were sampled, and by selecting the most proper concrete mixture design, PAC beams which corresponded to 0.6 m of a railway track were constructed. Finally, they were assessed in negative and positive loading in the beam midspan and in the positive sleeper rail seat according to EN13230-2 (2009) and in the negative sleeper rail seat according to AS 1085.14 (2019).

2 Mortar Tests

In this section, the consumed materials and the tests performed on mortar such as mortar fluidity time and compressive and flexural strength are separately presented.

2.1 Materials

2.1.1 Cement

The cement was ordinary Portland cement type 1–425 compliant with ASTM C150 (2015) whose specifications are listed in Table 2.

2.1.2 Sand

The sand was silica sand sourced from Firuzkuh mine (Iran). The range of the consumed sand combination should be selected such that it would not exceed the minimum and maximum grading ranges recommended in the ACI 304-1R (1997). The particle size distribution of individual sand codes, the consumed sand composition, and the permissible ranges of ACI are presented in Table 3 and Fig. 2. As recommended, either manufactured or natural sand may be used. The sand should be hard, dense, and durable, and contain uncoated rock particles. The grading in Fig. 2 should conform to ASTM C33 (2013). Fine aggregates that do not fall within these grading limits are useable. The selected sand composition comprises 35% of code D11, 50% of code 161, and 15% of code 181.

2.1.3 Water

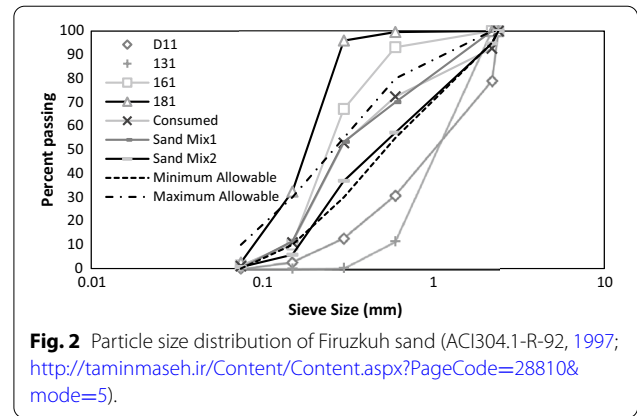
Ordinary tap water with a pH of 7 and a maximum temperature of 23 °C was utilized in accordance with ASTM D1193 (2011).

Table 2 Main specifications of Portland cement.

Main chemical components (%)										
	C ₃ S	C ₂ S	C ₃ A	C ₄ AF	CaSO ₄	Al ₂ O ₃	Fe ₂ O ₃	MgO	LOI	IR
	51	25	12.2	7.2	2.6	5.6	3.7	2.6	1.2	0.3
Physical properties										
References	Fineness (cm ² /g)	Retained on sieve #70 (%)	Autoclave expansion (%)	Normal consistency (%)	Setting time (min)		Compressive strength (MPa)			
					Initial	Total	3 days	7 days	28 days	
ASTM C204 (2016)	2528	10.95	0.56	25.1	175	245	15.6	23.6	43.1	
ASTM C136/C136M (2014)			ASTM C151/C151M (2016)	ASTM C187 (2016)	ASTM C191 (2013a)		ASTM C109/C109M (2013)			

Table 3 Main specifications of Firuzkuh sand (ACI304.1-R-92, 1997; <http://taminmaseh.ir/Content/Content.aspx?PageCode=28810&mode=5>).

Main chemical components (%)			
SiO ₂	Al ₂ O ₃	Fe ₂ O ₃	K ₂ O L.O.I
97.1	0.8	0.6	0.6
Physical properties			
Specific density (ton/m ³)		Humidity (%)	
D11	2.62	0.21	
NO.161	2.68		
NO.131	2.65		
NO.181	2.73		
Mohs hardness			7



2.1.4 Superplasticizer

The addition of a superplasticizer increases the grout fluidity even at low water/cement ratio (w/c) and consequently facilitates the effective filling of voids between aggregate particles. However, using an over dosage of a superplasticizer could increase bleeding, thus leading to excessive segregation of the sand in the grout mixture (Tang, 1977). The recommended dosage of superplasticizer for PAC normally ranges between (1.2–2% by cement weight) depending on its type (i.e., naphthalene sulphonate acid, polycarboxylate ester, etc.) (Abdelgader & Elgalhud, 2008; Abdul Awal, 1984; O'Malley & Abdelgader, 2010). In this study, superplasticizer was used as a chemical additive to provide a good level of fluidity and facilitate the injection procedure. In this matter, a polycarboxylate-based Superplasticizer with a specific density of 1.1 kg/m³ and a pH of 7 was used.

2.2 Mortar Test Plan

The mixing procedure of mortar components to produce 5 cm cubic specimens and 16 * 4 * 4-cm bending beams was performed according to the recommendation of ASTM standards of C305 and C511 (ASTM C305, 2014; ASTM C511, 2013). In addition, fluidity time of the mortars was measured using the ACI 304-1R (1997) recommendations. The fluidity time is a critical factor for mortar injection ability. By the laboratory trial and error method, the mortar with the maximum fluidity time of 70 s was identified as an injectable fresh mortar. If the fluidity time is >70 s, the mortar will not penetrate well into the ballast aggregates. The compressive strength of the mortar plays an important role in selecting and analyzing the best concrete mixture design. As recommended in ASTM C109 (2013), three cubic 5 * 5 * 5-cm specimens were utilized for this experiment, and the mean value of the compressive

strength of three specimens for each age and mixture design is presented. Flexural strength can be used to determine the tensile behavior of mortar. For this purpose, 16 * 4 * 4-cm beam specimens were constructed as recommended by ASTM C78 (2018) and C348 (2014). The results of the mean value of three specimens for each age and mixture design is presented. The presented results are the average values of three similar samples in each age and each mixture design. Samples were made in three cement contents of 750, 800, and 850 kg/m³, and two water-to-cement ratios (w/c) of 0.35 and 0.4. Each specimen was subjected to compressive and flexural strength tests at three ages of 1, 3, and 28 days, and their results are presented. The mortar test plan is listed in Table 4.

3 PAC Tests

After achieving the best mortar mixture designs, they were used to construct PAC beam samples by consuming suitable coarse-aggregate materials. Therefore, the railway ballast plays the role of coarse-aggregate concrete, generally because these materials are basically available in the railway track. Hence, the ballast was Grade 1 and 4 of the AREMA Code (American Railway Engineering and Maintenance-of-Way Association, 2012).

Table 5 and Fig. 3 present the characteristics and particle size distribution of ballast aggregates.

3.1 Developed Injection Apparatus

The ASTM C938 (2010) recommends the overall scheme of the mortar injection system for the construction of PAC as illustrated in Fig. 4 (A. C183, 2016). The injection system built in the laboratory environment consisted of three separate systems that could commence the injection procedure. These three systems included the mixing system (tank), the pressurized system, and the sampling system for injection molding and sample making. The mortar raw materials, including sand, cement, water,

and additives were first poured into the tank and then blended using a combination of engine, gearbox, shaft, and blade system. After the mortar was blended for a specified time and reached the desired level of fluidity, the discharge valve opened to let the mortar be poured into the pressurized system by gravity. The pressurized system was connected to the air pressure compressor via a valve (The pressure gauge could be contracted if the pressure drop had to be calculated). Once the compressor started to work, the mortar was ready to be injected into a cylindrical mold. The cylindrical mold had an inner diameter and height of 200 mm and 350 mm, respectively. Fig. 4 illustrates the entire scheme of the injection system.

3.2 PAC Test Plan

To achieve the best mixture design with the scope of the highest compressive strength of PAC, two types of ballast, Grade 1 and Grade 4 of AREMA code (American Railway Engineering and Maintenance-of-Way Association, 2012) whose specifications are given in Table 5 and Fig. 3, two types of sand mixes according to Table 6, and two w/c ratios of 0.35 and 0.4 were employed. The test schedule is given in Table 7.

Using the optimal mixture design and the highest values of compressive strength obtained in the preceding section, the beams were constructed using the PAC method. The beams were tested in two areas of sleeper midspan and rail seats in two conditions of the positive and negative applied moment in accordance with the European code EN13230.2 (2009). Each experiment was performed on three samples with the optimal mixture design obtained in the previous section after 28 days.

To simulate the track loading conditions in the laboratory and to perform a three-point bending test on the beam samples, it was necessary to make a beam of PAC with dimensions of 3 * 0.6 m and a height of 0.5 m to represent a sleeper spacing in railway tracks. The beam

Table 4 Mortar test plan.

Parameters	Test type																	
	Compressive strength (ASTM C109/C109M, 2013)			Flexural strength (ASTM C78/C78M, 2018; ASTM C348, 2014)			Fluidity test (ACI304.1-R-92, 1997)											
Cement content (kg/m ³)	750			800			850			750			800			850		
Age (day)	Number of constructed specimens												Number of tests on fresh mortar					
	w/c																	
	0.35	0.4	0.35	0.4	0.35	0.4	0.35	0.4	0.35	0.4	0.35	0.4	0.35	0.4	0.35	0.4	0.35	0.4
1	3	3	2	3	4	3	Impossible	4	Impossible				3	3			4	
3	4	3	4	4	4	4												
28	3	3	3	4	3	3												

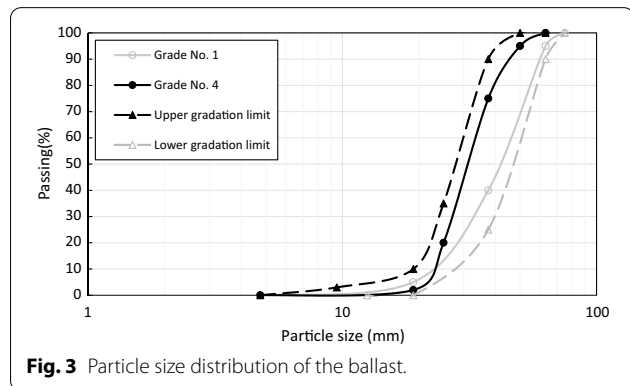


Fig. 3 Particle size distribution of the ballast.

a sleeper-excluded (SE) PAC beam was first constructed, and in accordance with Fig. 8a, the flexural strength of the SE beam was measured. After achieving the flexural strength of the SE beam, the SPM test was performed to determine the positive bending behavior of the PAC beam and sleeper, and measure the positive bending capacity of the PAC beam. This test was conducted using the European Regulations EN13230 (2009) and in accordance with Fig. 8b.

In the figure above, F_{C_0} stands for the initial positive reference force at the center of the beam, F_{C_r} represents the positive force at the center of the beam when the first crack is created, and F_{C_b} denotes the maximum positive force applied to the beam without increasing it. Initially, the loading procedure increased with the rate of 120 kN/

Table 5 Physical characteristics of the ballast.

Type	Specific weight (ton/m ³)	Los Angles abrasion (%)	Micro-deval abrasion (%)	Water absorption (%)	Point load index (MPa)		Uniaxial compressive strength (MPa)
					Uncorrected	Corrected	
Andesite	2.26	13	18.8	1.34	8.82	7.60	158.7

mold consisted of a transparent side. The gravity injection method was used to make the sample of the PAC beam; the ballast aggregates were first poured into the sample mold, and then, the mortar was poured onto the ballast surface soon after the sleeper was put on the ballast. To prevent mortar waste, all mold joints were sealed using a string of rubber tape. Plastic was also used inside the mold to prevent the concrete from adhering to the mold walls. Fig. 5 depicts the scheme of beam construction. To assess the flexural behavior of the PAC beam, it is essential to investigate its behavior in the case of sleeper exclusion (SE). For this purpose, after constructing the PAC beams, the exerted vertical load and the related deflection were, respectively, logged by a load cell and LVDT. Subsequently, by assessing the flexural strength of the pure beam (SE), the sleeper-included beam was constructed and the beams were tested in four modes of SPM, SNM, SPR, and SNR, and the results are addressed in the following subsections. In total, three specimens without a sleeper and 12 specimens with a sleeper for positive and negative bending moment tests of the beam in both midspan and rail seat were made (Fig. 8). The loading method and the load-deformation results are given in the following sections.

3.2.1 SE and SPM Tests

Fig. 6 displays the loading steps of the bending test in SE and SPM tests according to EN13230 (2009). To perform the tests on the PAC beam and to measure its strengths,

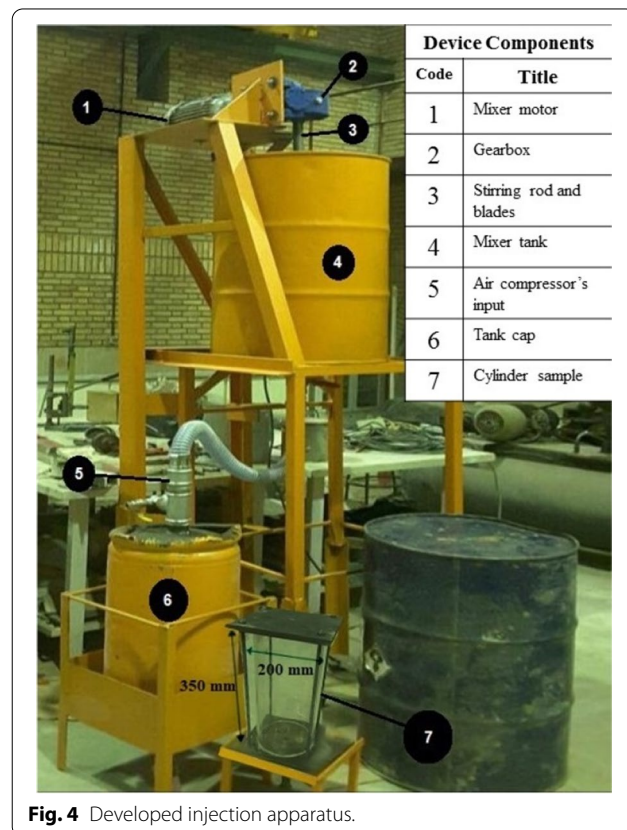


Fig. 4 Developed injection apparatus.

Table 6 Sand.

Sand mix	Sand type			
	D11	131	161	181
Sand mix 1	0%	30%	50%	20%
Sand mix 2	25%	25%	50%	0%

Table 7 PAC test plan.

w/c	Ballast grade	Sand mix
0.4	Ballast grade 1	Sand mix 1
0.35	Ballast grade 4	
0.4	Ballast grade 1	Sand mix 2
0.35	Ballast grade 4	
0.4	Ballast grade 1	

min to reach the F_{c0} ; then, the loading continued with the steps of 5 kN in a duration of 10 s to 5 min each to attain the beam failure.

3.2.2 SNM Test

This test was conducted using the European Regulations EN13230 (E. B., 2009) and in accordance with Fig. 8c. This test was performed to determine the negative bending behavior of the PAC beam and sleeper, and measure

the negative bending capacity of the PAC beam. The loading steps were applied, as shown in Fig. 6.

3.2.3 SPR Test

This test was performed to elucidate the positive flexural strength of the rail support on the concrete beam with a sleeper if the load entered the rail seat. The test was conducted based on the European Code EN13230 (E. B., 2009):

$$F_{r0} = \frac{4M_{dr}}{L_r - 0.1} \tag{1}$$

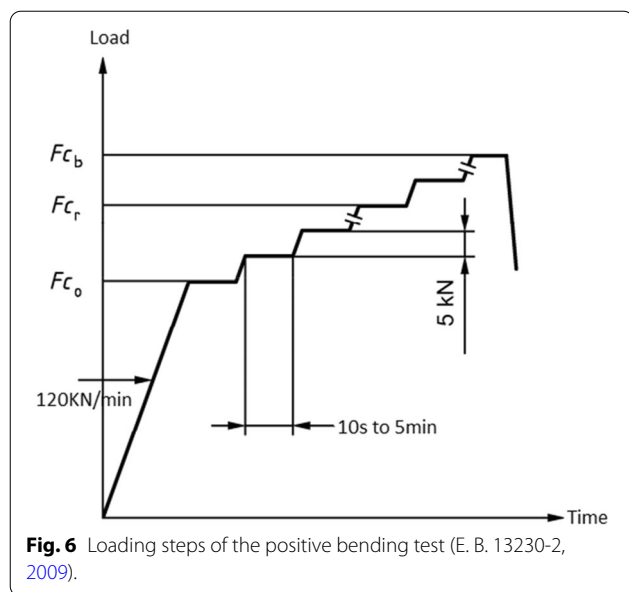
where F_{r0} is the initial force required to conduct the test in kN, M_{dr} is the flexural moment design of the rail seat in kN m, and L_r is in m. Since $L_p < 0.45$, then the L_p value is 0.6. The test layout was in accordance with Fig. 8d, and the values of L_r and L_p are defined in Fig. 7. Accordingly, L_r is the bearing spacing and L_p represents the distance of the loading location from the external edge of the beam.

3.2.4 SNR Test

The experiment is not defined in European regulations but was conducted to obtain the negative bending resistance of the rail seat (Australia Standard, 2003). The arrangement of this test was performed in accordance with Fig. 8e, and the loading steps were carried out according to the positive vertical load test of the European Rail Seating Area EN13230 (2009) which is described in Fig. 6.



Fig. 5 Casting of PAC beam before and after mortar injection: (Right) before injection, (Left) after injection.



3.3 PAC Beams Instrumentation

After pouring the ballast into the sample and constructing the concrete, it was time to prepare it for loading. To do this, the LVDT was inserted in the middle part of the beam; then, the load sensor was placed on the concrete sample, and the hydraulic jack was placed over the load gauge. Afterwards, as depicted in Fig. 8, the LVDT and load gauge were connected to the data logger and the computer to read the output data by the corresponding wires.

4 Results and Discussion

4.1 Mortar Test Results

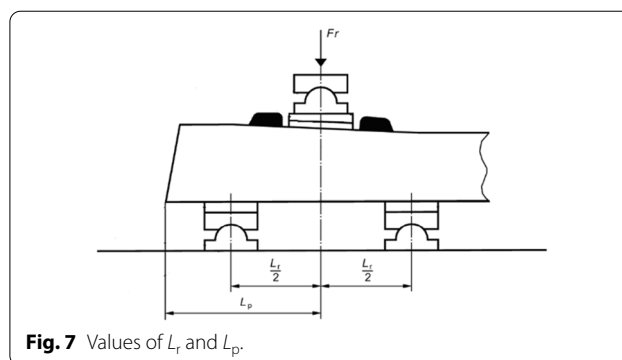
The results obtained from tests on the mortar are discussed in the subsections below.

4.1.1 Fluidity Time

The results of the flow evaluation of the specimens to which the superplasticizer was added are illustrated in Fig. 9. Only samples with a water-to-cement ratio of 0.4 could be injected. The maximum allowable fluidity time was determined as 70 s by trial and error. This means that fresh mortars having a fluidity time < 70 s were injectable; otherwise, the mixture design had to be modified and rewritten.

4.1.2 Compressive Strength

At a water-to-cement ratio of 0.35 for the cement content of 750 kg/m^3 , the injecting of mortar was virtually impossible; therefore, the results were discarded. Fig. 10 depicts the compressive strength of the selected mortars at three ages.



Mortars averagely attained at least 80% of their ultimate strength in the first 3 days. Moreover, as the water-to-cement ratio increased, the compressive strength decreased, and at 28 days, a greater compressive strength occurred at a higher cement content and lower water-to-cement ratio. It can be concluded that the introduced mortars individually addressed large values of compressive strength without using additives. The bending behavior of the mortar shall be investigated if it is to be consumed into the PAC slab.

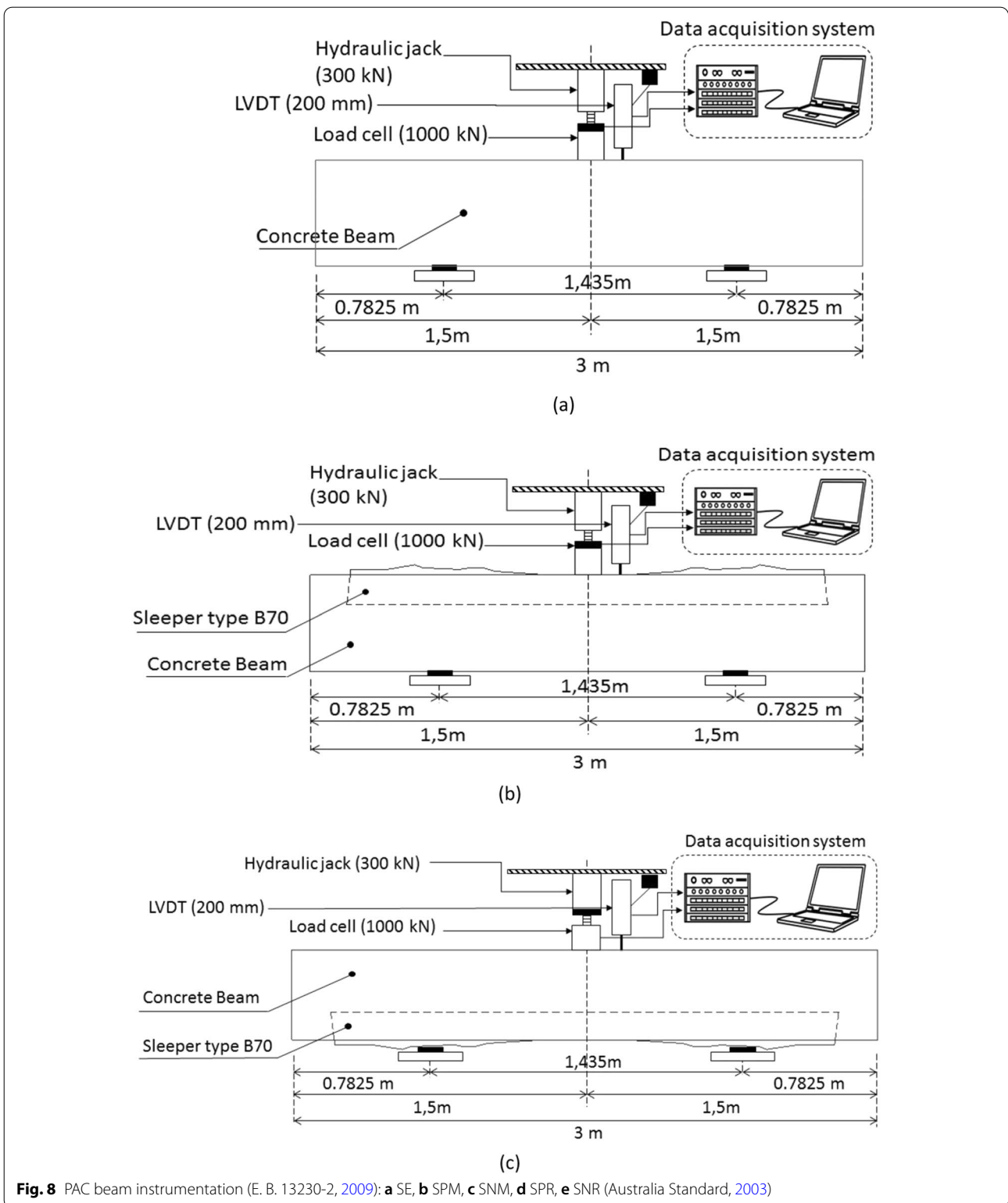
4.1.3 Flexural Strength

Fig. 11 presents the results of performing a three-point flexural strength test on the mortar samples. As expected, the highest flexural strength occurred at a lower water-to-cement ratio. In addition, due to the small value of 1-day flexural strength, the values for all such mortars were set to zero. The diagram shows that the introduced mortars demonstrated a proper flexural strength. Therefore, the utilized sand and cement were both used for constructing PAC slabs.

4.2 PAC Test Results

After injection and sample processing, the uniaxial compressive strength test was performed at 1, 3, and 28 days (Fig. 12). The results of these experiments are given in Fig. 13. For ensuring the accuracy of the results, three cylindrical specimens had to be broken for each mixture design and age.

Based on Fig. 13, Grade 1 of ballast aggregates demonstrated higher values of compressive strength due to their inherent strength provision characteristic for their large aggregate sizes. Laboratory tests were performed using the fifth mixture design with a water-to-cement ratio of 0.4 and a 28-day compressive strength of 16.4 MPa. This was done for not using the injection apparatus for the construction of beams. As expected, by lowering the w/c ratio, the compressive strength of the specimen



increased. On the other hand, increasing the aggregate dimension maximized the compressive strength. Because the force was directly imposed on the ballast aggregates,

a higher force was required to break the larger aggregates. In addition, by enlarging the sand dimensions, the mortar compressive strength increased due to the filling

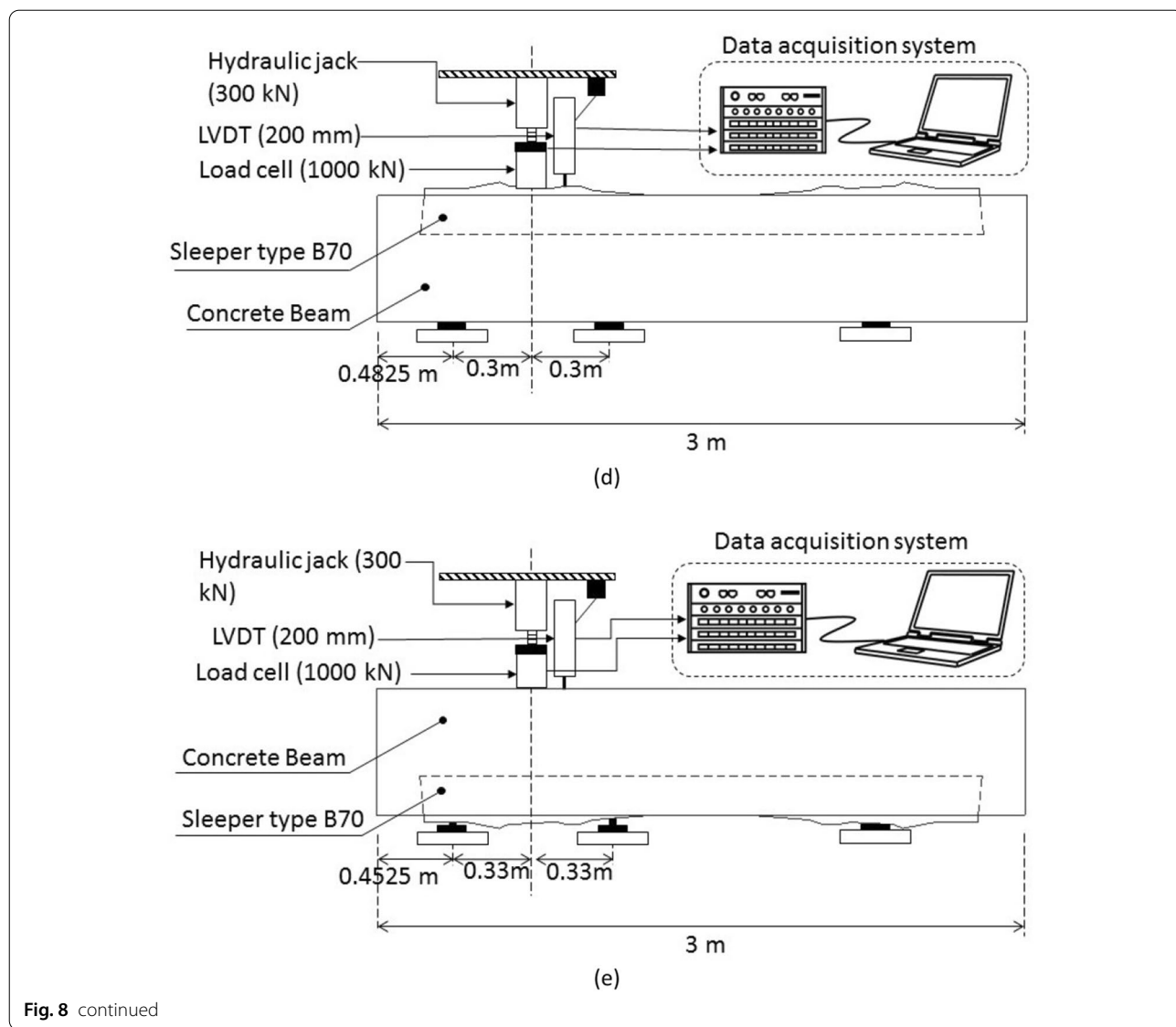


Fig. 8 continued

of porosity imprisoned between the ballast aggregates. This prevented crack growth in the mortar and transmitted the applied force to the ballast aggregates.

4.3 PAC Beams Test Results

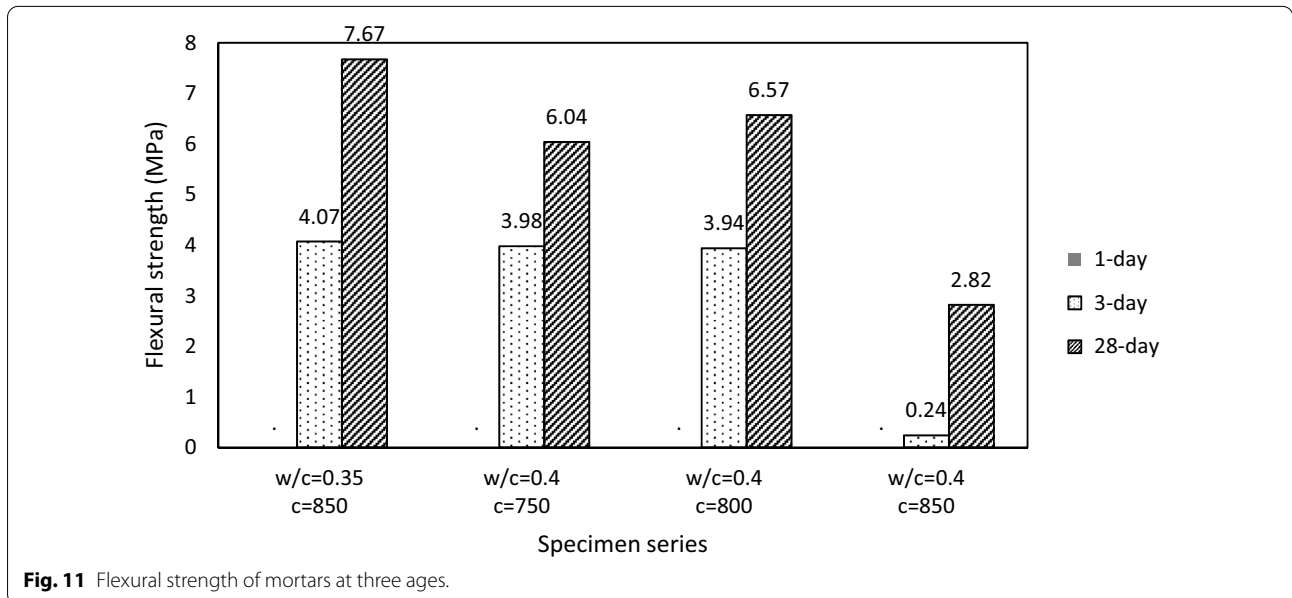
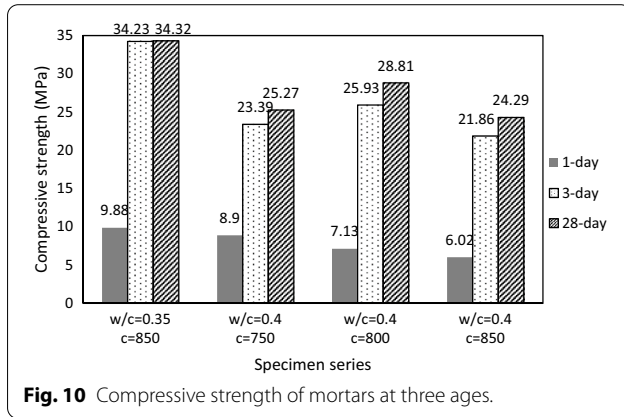
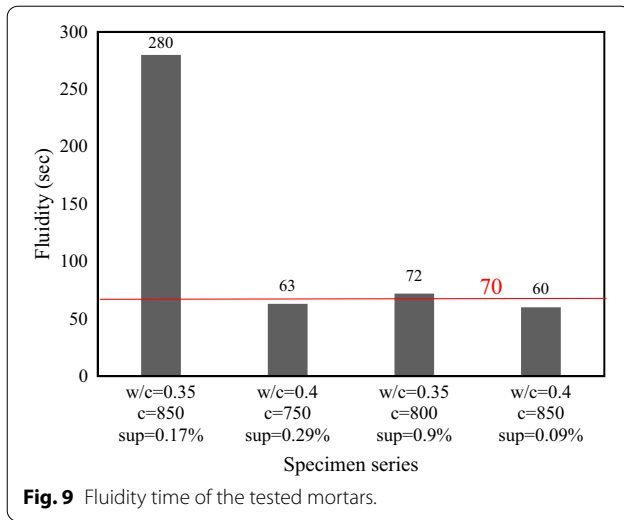
In this section, the results of beam specimens with ballast grade 1, sand mix 2, and a w/c of 0.4 with superplasticizer consumption of 0.29% cement weight are separately addressed. This combination was used in order to satisfy both requirements of ease of sampling and obtaining a high strength.

4.3.1 SE Results

The result of the bending test of the concrete beam without a sleeper is depicted in Fig. 14. A sleeper-excluded

PAC beam tolerates 177.5 kN of bending force applied to the center of the beam until it fails. After analyzing the beam based on the equations in ACI 318 (2011), it was found that the load required for the failure of the concrete beam with dimensions of 3 * 0.6 * 0.5 m is 171.62 kN, which is less than the results obtained from the presented test.

As depicted in Fig. 15, the beam passed its elastic area without generating cracks. At the deflection of about 2 mm, a crack was generated into the PAC beam, but because of the interaction of ballast aggregates (from a beam section standpoint), the beam did not completely fail. Eventually, by applying higher forces at the deflection of about 2.5 mm, the beam completely failed. This



proved the beam's brittle nature in the case of excluding the sleeper.

4.3.2 SPM Results

Fig. 16 presents the result of the sleeper-included positive bending moment of the midspan.

A force of 151.02 kN was first applied until the PAC failed (Fig. 16) at the deflection of 0.51 mm (point A), which was less than the maximum bending force tolerated by pure concrete beams. The exerted load dropped until 88.26 kN (point B) at which the sleeper started to endure the jack loading. The increasing trend continued until the sleeper completely broke at the force of 150.04 kN (point C) and the entire beam collapsed (point D). Thus, the maximum amount of moment tolerated by PAC was determined as 55.25 kN m. The maximum positive moment value created in the middle of the sleeper was calculated using the 25-ton train axial load, the LM71 load distribution model, and the dynamic impact coefficient obtained by AREMA (2012), in the form of the equations below:

$$\phi = 1 + 5.21 \frac{V}{D} \tag{2}$$

where V is the train speed (considered to be 160 km/h) and D is the radius of the wheel (equal to 914 mm):

$$M_{c+} = 0.05q_r(l - g) \tag{3}$$

where q_r denotes the wheel load multiplied by the impact factor calculated using Eq. 2, which was computed as 117.68 kN, l represents the length of the sleeper which



Fig. 12 PAC cylindrical specimens under uniaxial compressive load: (Right) cylindrical specimen, (Middle) crack growth during loading, (Left) failure.

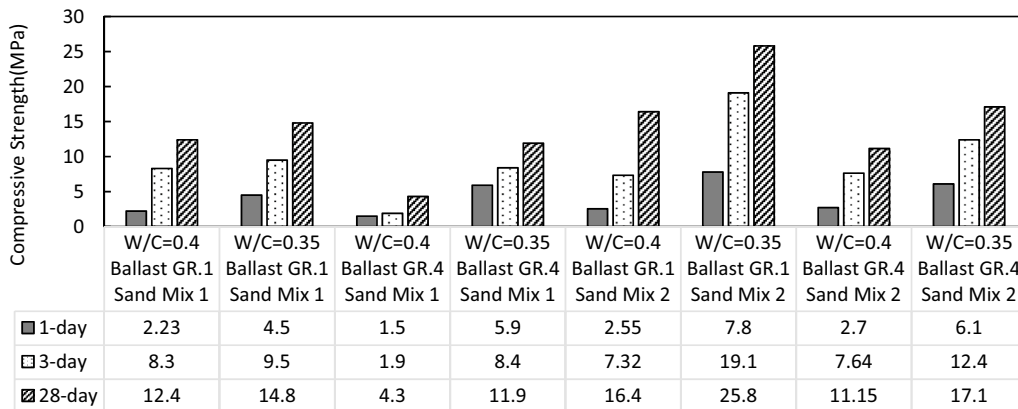


Fig. 13 PAC compressive strength at three ages.

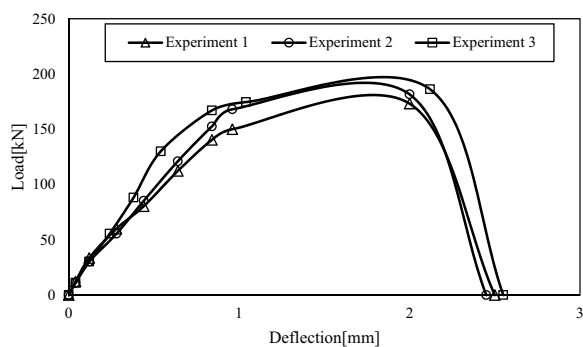


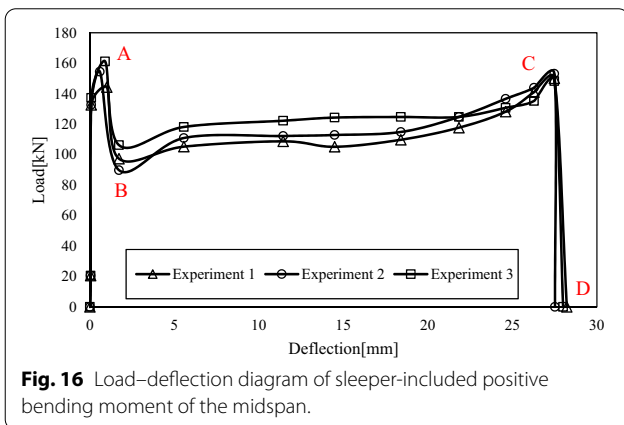
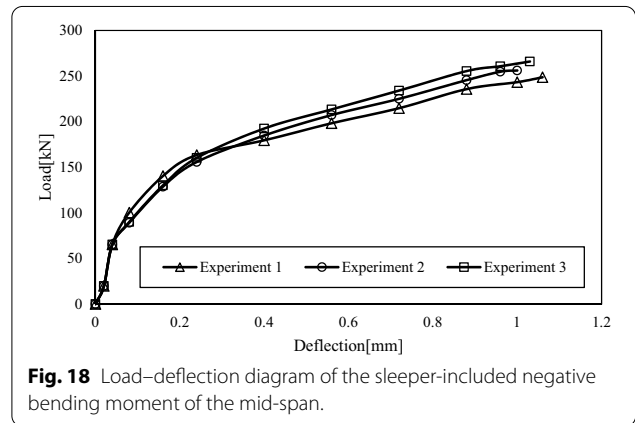
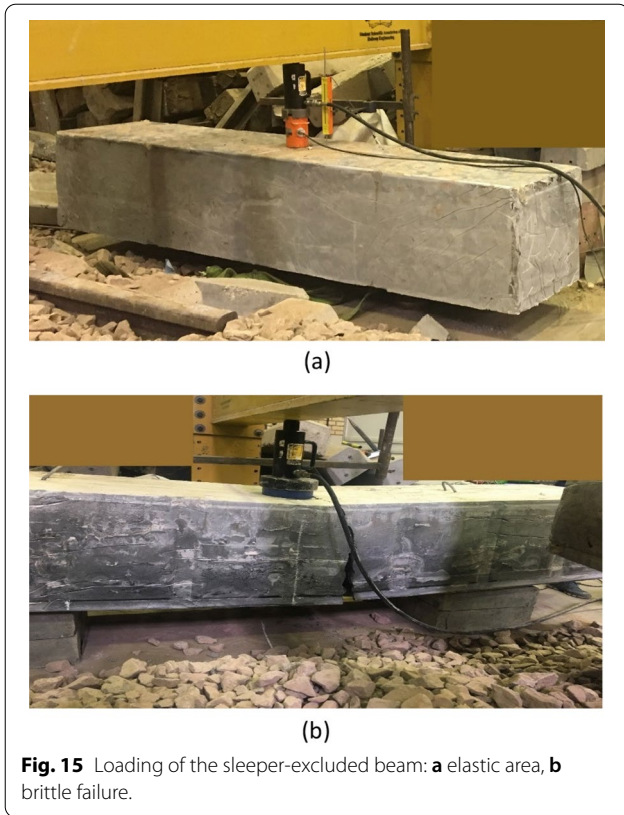
Fig. 14 Load–deflection diagram of the sleeper-excluded beam.

is (2.6 m), and g is the axis-to-axis length of the rail seat (1.5 m).

It is concluded that the maximum amount of moment generated is 6.39 kN m which is much less than the positive moment tolerated by the concrete beam. Fig. 17 shows the PAC failure in the first step of load application in SPM tests.

4.3.3 SNM Results

Fig. 18 shows the sleeper-included negative bending moment diagram of the midspan.



The diagram shows that, initially, until the force of about 68.65 kN, the load was just applied to PAC and the embedded sleeper, and the beam behavior was completely fragile. Then, with the interaction of reinforcements of the sleeper, the beam behavior switched to ductile, and therefore, the diagram slope decreased. The PAC beam withstood 251.05 kN of force as a negative bending moment in the center of the beam with a sleeper, and no cracks were observed. This amount of force

generated a moment of 91.84 kN m in the middle of the beam. The maximum negative anchor value generated in the middle of the sleeper is calculated using the 25-ton train axial load, the LM71 load distribution model, and the dynamic impact coefficient obtained by AREMA (2012) by Eq. 2:

$$M_{c-} = q_r \left(\frac{2g - l}{4} \right) \tag{4}$$

where q_r is the maximum negative moment (14.1 kN m), l is the length of the sleeper which is (2.6 m), and g is the axis-to-axis length of the rail seat (1.5 m).

4.3.4 SPR Results

The sleeper-included positive bending moment diagram of the rail seat is illustrated in Fig. 19.

Initially, with applying the force on both sleeper reinforcement and PAC, the beam behavior was ductile;

on average, the sleeper-included PAC beam tolerated 214.76 kN of positive vertical force at the rail seat, and no cracks were observed. This load is equal to 117.68 kN for a 25-tons passing train and, according to the impact factor calculated by Eq. 2, it is about 2 times as tolerable as that shown in the diagram. This amount of force generated a positive moment of 32.5 kN m at the rail seat location:

$$M_{R+} = q_r \left(\frac{l-g}{8} \right) \tag{5}$$

in which q_r is the maximum negative moment (14.1 kN m), l is the length of the sleeper which is (2.6 m), and g is the axis-to-axis length of the rail seat (1.5 m).

The maximum positive value generated at the sleeper support obtained by this equation is equal to 15.97 kN, which is much less than the positive moment tolerated by PAC beams.

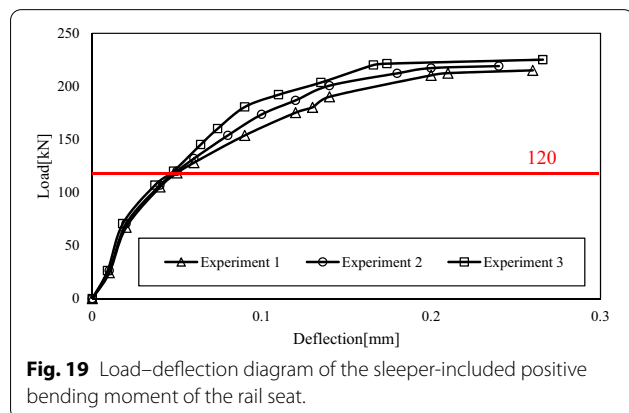
4.3.5 SNR Results

The result of the sleeper-included negative bending moment diagram of the rail seat is displayed in Fig. 20.

The concrete sleeper beam tolerated on average 227.12 kN of negative vertical force at the negative location of the rail seat; both PAC and the embedded sleeper remained in a linear state; and no cracks were observed. This amount of force generated a moment of 38.21 kN m at the negative location of the rail seat in the beam. This value is calculated using the 25-ton train axial load, the LM71 load distribution model, and the dynamic impact coefficient Eq. 2:

$$M_{R-} = \text{Max}\{0.67M_{R+}, 14\} \tag{6}$$

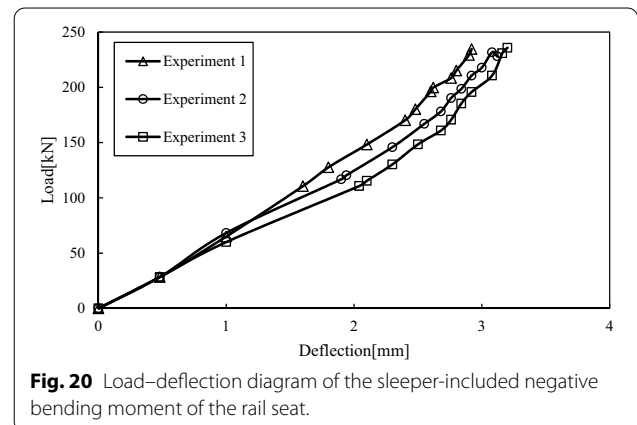
Based on Eq. 6, the maximum negative moment value created at the sleeper test is equal to 14 kN m, which is much less than the negative moment tolerated by PAC beams.



5 Conclusion

To investigate the flexural behavior of a PAC beam using ballast materials, an optimal mixture was first obtained using the mortar results of fluidity time, compressive and flexural strength. In the next step, with the development of the injection apparatus, the concrete specimens were constructed using the former mixture design. Afterwards, by constructing the concrete beams using PAC technology in two modes of with and without a sleeper, bending moment tests were performed on the beams. The most important results are as follows:

- By changing the water-to-cement ratio in the mortar in the range of 0.3 to 0.5, the best-recommended fluidity time for the injectable mortar specimens was at least 70 s. The highest values of compressive and flexural strength of mortar at the water-to-cement ratio of 0.4 with 800 kg/m³ of cement content were obtained as 7.13 and 0 MPa for 1 day, 25.93 and 3.94 for 3 days, and 28.88 MPa and 6.57 MPa for 28 days, respectively.
- The highest compressive strength of the concrete specimen without the need for injection apparatus was obtained at the water-to-cement ratio of 0.4, sand composition of 2 (25% D11 sand, 25% sand 131, and 50% sand 161), and ballast grade 1, which possessed a 1-day compressive strength of 2.55 MPa, 3-day 7.32 MPa, and 28-day 16.4 MPa. According to the studies conducted on the 25MGT (million gross tons which annually pass through the track) axial load train, the minimum compressive strength required based on the numerical analysis performed by these authors was 13 MPa to satisfy the design requirements.
- The maximum bending force in the non-sleeper concrete beam midspan was 177.5 kN, which is higher



than the breakdown achieved by ACI318, reported as 171.62 kN.

- In sleeper-included beams, the maximum force tolerated by PAC was 151.02 kN, while the sleeper tolerated 150.04 kN, and then complete failure occurred. This is less than the fracture force obtained by non-sleeper concrete beams, which is 177.5 kN, due to the use of sleepers in the construction of PAC beams and the decrease in the height of concrete beams. This force generated a moment of 55.25 kN m in the PAC beam, which is much larger than that generated by a 25-ton axle train. Moreover, the maximum force applied to the positive sleeper rail seat was 214.76 kN, which generated 32.5 kN m in the PAC beam, much larger than the moment suggested in the AREMA code.
- The maximum force applied at the negative bending center of the sleeper-included PAC beam and the maximum force applied at the vertical negative location of the PAC beam rail seat equaled 251.05 and 227.12 kN, which generated the moments of 91.84 kN m and 38.21 kN m, respectively. These values are much larger than the moment generated by the 25-tons axial freight train according to the relations in AREMA.

Authors' Contributions

ME: supervising, test planning, results analyzing, and paper writing–editing.
HA: conducting the tests, instrumentations, data gathering, and writing the paper. Both authors read and approved the final manuscript.

Authors' Information

M.E: Full time Professor of School of Railway Engineering, Iran University of Science and Technology; H.A: Graduated in M.sc of Railway Track Engineering, School of Railway Engineering, Iran University of Science and Technology.

Funding

The authors have not received any funding from anywhere for doing the research.

Availability of Data and Materials

Some or all data, models, or code that support the findings of this study are available from the corresponding author upon reasonable request.

Declarations

Competing Interests

The authors declare that they have no competing interests.

Received: 15 July 2021 Accepted: 2 December 2021

Published online: 21 February 2022

References

A. C183. (2016). *Standard practice for sampling and amount of testing of hydraulic cement*. West Conshohocken: ASTM International.

- A.C33/C33M. (2013). *Standard specification for concrete aggregates*. West Conshohocken: ASTM International.
- Abdelgader, H. S., El-Baden, A. S., Abdurrahman, H. A., Awal, A. S. M. A. (2018). *Two-stage concrete as a sustainable production*. Presented at the MATEC Web of Conferences 149.
- Abdelgader, H. S., & Elgalhud, A. (2008). Effect of grout proportions on strength of two-stage concrete. *Structural Concrete*, 9(3), 163–170.
- Abdelgader, H. S., & Górski, J. (2003). Stress-strain relations and modulus of elasticity of two-stage concrete. *Journal of Materials in Civil Engineering*, 15(4), 329–334.
- Abdelgader, H., Najjar, M., & Azabi, T. (2010). Study of underwater concrete using two-stage (preplaced aggregate) concrete in Libya. *Structural Concrete*, 11(3), 161–165.
- Abdul Awal, A. (1984). *Manufacture and properties of prepacked aggregate concrete*.
- ACI304.1-R-92. (1997). *Guide for the use of preplaced aggregate concrete for structural and mass concrete applications*. Farmington Hills: American Concrete Institute.
- ACI318. (2011). *Building code requirements for structural concrete and commentary*.
- American Railway Engineering and Maintenance-of-Way Association. (2012). *Roadway and ballast*. Washington, DC: American Railway Engineering and Maintenance-of-Way Association.
- AS 1085.14. (2019). *Railway track material, Part 14: Prestressed concrete sleepers*.
- ASTM. (2010). *ASTM C938–80: Standard practice for proportioning grout mixtures for preplaced-aggregate concrete*. West Conshohocken: ASTM International.
- ASTM C109/C109M. (2013). *Standard test method for compressive strength of hydraulic cement mortars*. West Conshohocken: ASTM International.
- ASTM C136/C136M. (2014). *Standard test method for sieve analysis of fine and coarse aggregates*. West Conshohocken: ASTM International.
- ASTM C150/C150M. (2015). *Standard specification for portland cement*. West Conshohocken: ASTM International.
- ASTM C151/C151M. (2016). *Standard test method for autoclave expansion of hydraulic cement*. West Conshohocken: ASTM International.
- ASTM C187. (2016). *Standard test method for amount of water required for normal consistency of hydraulic cement paste*. West Conshohocken: ASTM International.
- ASTM C191. (2013a). *Standard test methods for time of setting of hydraulic cement by Vicat needle*. West Conshohocken: ASTM International.
- ASTM C204. (2016a). *Standard test method for fineness of hydraulic cement by air-permeability apparatus*. West Conshohocken: ASTM International.
- ASTM C305. (2014). *Standard practice for mechanical mixing of hydraulic cement pastes and mortars of plastic consistency*. West Conshohocken: ASTM International.
- ASTM C348. (2014b). *Standard test method for flexural strength of hydraulic-cement mortars*. West Conshohocken: ASTM International.
- ASTM C511. (2013). *Standard specification for mixing rooms, moist cabinets, moist rooms, and water storage tanks used in the testing of hydraulic cements and concretes*. West Conshohocken: ASTM International.
- ASTM C78/C78M. (2018). *Standard test method for flexural strength of concrete (using simple beam with third-point loading)*. West Conshohocken: ASTM International.
- ASTM D1193. (2011). *Standard specification for reagent water*. West Conshohocken: ASTM International.
- Australian Standard. (2003). *Railway track material, Part 14: Prestressed concrete sleepers*. Australian Standard: AS1085. 14-2003.
- Coo, M., & Pheerapahn, T. (2015). *Effect of sand, fly ash, and coarse aggregate gradation on preplaced aggregate concrete studied through factorial design*. Amsterdam: Elsevier.
- E. B. 13230-2. (2009). *Railway applications-track-concrete sleepers and bearers*. British Standards Institution.
- Hagio, Y. (2011). *Project evaluation and future work of TC type low-maintenance track*. Tokyo: EAST Japan Railway Company.
- Lee, S., et al. (2018). Effects of redispersible polymer powder on mechanical and durability properties of preplaced aggregate concrete with recycled railway ballast. *International Journal of Concrete Structures and Materials*, 12(1), 69.
- Mohammadhosseini, H., Tahir, M. M., Alaskar, A., Alabduljabbar, H., & Alyousef, R. (2020). Enhancement of strength and transport properties of a novel

- preplaced aggregate fiber reinforced concrete by adding waste polypropylene carpet fibers. *Journal of Building Engineering*, 27, 101003.
- Najjar, M., Soliman, A. M., & Nehdi, M. L. (2014). Critical overview of two-stage concrete: Properties and applications. *Construction and Building Materials*, 62, 47–58.
- Najjar, M., Soliman, A., & Nehdi, M. (2016). Two-stage concrete made with single, binary and ternary binders. *Materials and Structures*, 49(1–2), 317–327.
- Najjar, M. F. (2016). *Innovating two-stage concrete with improved rheological, mechanical and durability properties*.
- O'Malley, J., & Abdelgader, H. S. (2010). Investigation into viability of using two-stage (pre-placed aggregate) concrete in Irish setting. *Frontiers of Architecture and Civil Engineering in China*, 4(1), 127–132.
- Rajabi, A. M., & Moaf, F. O. (2017). Simple empirical formula to estimate the main geomechanical parameters of preplaced aggregate concrete and conventional concrete. *Construction and Building Materials*, 146, 485–492.
- Rajabi, A. M., Omid Moaf, F., & Abdelgader, H. S. (2020). Evaluation of mechanical properties of two-stage concrete and conventional concrete using nondestructive tests. *Journal of Materials in Civil Engineering*, 32(7), 04020185.
- Retrieved from, <http://taminmaseh.ir/Content/Content.aspx?PageCode=28810&mode=5>.
- Takahashi, T., Itou, K., & Fuchigami, S. (2012). Development of pre-packed concrete trackbed for Shinkansen. *Railway Technical Research Institute Report*, 26(2), 19–24.
- Tang, C. (1977). *Properties of prepacked concrete*. University of Melbourne.

Publisher's Note

Springer Nature remains neutral with regard to jurisdictional claims in published maps and institutional affiliations.

Submit your manuscript to a SpringerOpen[®] journal and benefit from:

- ▶ Convenient online submission
- ▶ Rigorous peer review
- ▶ Open access: articles freely available online
- ▶ High visibility within the field
- ▶ Retaining the copyright to your article

Submit your next manuscript at ▶ [springeropen.com](https://www.springeropen.com)
